# GPU-ACCELERATED SAR IMAGE FORMATION IN THE PRESENCE OF VERY LARGE MOTION ERROR

Andrew Willis, Christopher Beam

Garrett Demeyer, Kevin Brink

University of North Carolina at Charlotte
Dept of Electrical and Computer Engineering
Charlotte, NC 28223-0001
{cbeam18, arwillis}@uncc.edu

Air Force Research Laboratory

Munitions Directorate

Eglin AFB, FL, 32542

{garrett.demeyer.1, kevin.brink}@us.af.mil

#### ABSTRACT

Synthetic Aperture Radar (SAR) systems sense electromagnetic backscatter from scenes generated from a sequence of excitation pulses of RF radiation emitted from the radar antenna varying spatial positions. Focusing the radar returns into coherent images requires highly accurate knowledge of the antenna position for the duration of the pulses. In this article a massively parallel approach is propose to solve the NP-hard problem of focusing radar data collected in the presence of large motion errors. Little research has been dedicated to the development of focusing algorithms capable of image formation when motion error magnitudes exceed the nominal wavelength of the radar excitation signal. This problem has been shown to be non-deterministic polynomial-time hard (NP-hard) to solve and computational challenges are exacerbated by the high computational cost of associated with the SAR focusing algorithms needed to conduct the search. The proposed approach seeks to address these challenges by restricting trajectories to smooth (low-order) curve trajectories and applying an optimized massively parallel GPU implementation of the SAR focusing algorithm to search over candidate trajectories for the trajectory yielding a focused SAR image.

### 1 Introduction

Synthetic Aperture Radar (SAR) systems typically employ a method of sensing electromagnetic backscatter by illuminating a scene with a sequence of RF radiation pulses emitted from various spatial positions. In the case of monostatic SAR measurement contexts, a single high-power RF antenna is utilized as both an emitter and a receiver of RF signals. It transmits the RF excitation pulses and captures the RF backscatter from the scene. The nominal RF operating wavelength of the antenna,  $\lambda$ , is a determining factor in the image resolution and whether the radar is able to penetrate terrestrial surfaces and atmospheric phenomena, e.g., C-band (surface/ground penetrating), L-band (canopy penetrating), X-band (smoke/cloud/rain penetrating).

SAR image formation is very sensitive to position error,  $\epsilon$ , and when the error exceeds 10% of the nominal operating RF wavelength,  $\lambda$ , SAR focusing algorithms fail to generate coherent images [1, 2].

This article describes a massively parallel approach to solve the NP-hard problem of focusing radar data collected in the presence of excessively large motion errors, i.e., in contexts where  $|\epsilon|\gg \lambda/10$ . Successful deployment of such algorithms promises to allow Synthetic Aperture Radar (SAR) systems to be deployed onto low-cost INS vehicle platforms and in the absence of highly accurate GPS information. The (2) contributions to this article are: (1) an approach to focus SAR images in the presence of large motion errors and (2) a massively-parallel procedure using GPU acceleration to search over the unknown trajectories in a short time.

## 2 Related Work

SAR images are constructed using focusing algorithms [3, 4, 5, 6] that serve to merge the local measurements of the scene from each position into a single coherent image. To do so, highly-accurate measurements of the antenna positions at time each pulse is emitted must be known [7, 8].

Many SAR system use RF frequencies with wavelengths on the order of  $\lambda=3cm$ . or smaller. This requires the position accuracy required for coherent SAR image formation to satisfy the inequality  $|\epsilon|<3mm$ . which is demanding for spatially large trajectories where turbulence of INS error can spoil image formation. This constraint on the accuracy of the vehicle position requires SAR platforms to be constructed with highly accurate position sensors which typically realize as a high-resolution GPS receiver and a high-accuracy INS (Inertial Navigation System).

Little research has been dedicated to the development of focusing algorithms capable of image formation for large magnitude motion error, i.e.,  $|\epsilon|\gg \lambda/10.$  A major impediment to development of such algorithms is that the problem of SAR focusing under these conditions is non-deterministic polynomial-time hard (NP-hard) as it requires finding a solu-

tion (typically a local optimal point) to a (NP-hard) optimization problem [2]. Auto-focus algorithms have been discussed in [1, 2, 9, 10] where such algorithms seek to correct motion error to improve SAR image quality. However auto-focus algorithms such as [2, 10] do not address large-scale motion errors such as contexts where  $|\epsilon| \gg \lambda/10$ .

# 3 Methodology

This work considers the problem of SAR trajectory motion compensation by seeking to estimate the vehicle trajectory that yields a coherent SAR image. A purpose-built massively parallel grid search algorithm accelerates consideration of potential candidate trajectories by considering solution trajectories in parallel and by computing SAR focusing algorithm results in parallel.

The proposed approach consists of three steps: (1) choose a model to parameterize the trajectory, (2) define a performance functional that indicates the likelihood a given trajectory model is correct, (3) define the search space limits and find the best solution within that space using massively-parallel grid search.

# 3.1 Choosing a trajectory parameterization model

To save computational cost, positions of the vehicle over the aperture are considered to lie along a smooth curve. We adopt a 3D polynomial space curve model for trajectory and investigate  $1^{st}$  and  $2^{nd}$  order, i.e., linear and quadratic. These reduced order models are appropriate in practice since most SAR measurements are taken with linear (stripmap) or circular (spotlight) trajectory geometry. The reduced order model serves to minimize the dimension of the search space which is crucial in controlling the computational cost of the approach.

Equation (1) shows the form of the parametric 3D space curve model which represents variation along each coordinate system axis as an algebraic polynomial function of the curve arc length, s.

$$C(X(s), Y(s), Z(s)) = (\sum_{k=0}^{K} \alpha_k s^k, \sum_{k=0}^{K} \beta_k s^k, \sum_{k=0}^{K} \gamma_k s^k)$$
(1)

Our experiments consider linear (K=1) and quadratic (K=2) models for equation (1). SAR RF pulse emission positions are realized as regularly spaced samples having interval, T, along the arc-length curve as determined by the SAR Pulse Repetition Frequency (PRF). A final parameter allows the vehicle velocity to vary by addition of a single parameter v that multiplies the sample interval resulting in samples with spacing vT. The resulting space curve model therefore includes both a vehicle velocity and vehicle trajectory shape considerations which we refer to collectively as the  $trajectory\ model$ .

#### 3.2 Defining the performance functional

Values of the performance function for each candidate trajectory model are obtained via a 2-step process: (1) focus the SAR image using the candidate trajectory and the back projection algorithm [3, 11] and (2) use the column entropy metric as shown in equation (2) to evaluate the focused image quality. This metric has been found to be an appropriate for detecting correct vehicle trajectories.

$$H(Y|\alpha_k) = \sum_{y \in \mathcal{Y}} p(y|\alpha_k) \log p(y|\alpha_k)$$
 (2)

Maxima of the column entropy are indications of potentially correct trajectory models.

### 3.3 Performing the search for a solution

Vehicle trajectory/velocity paths are then modeled as points in 7-dimensional space for linear trajectories and as points in 10-dimensional space for quadratic trajectories. A massively parallel GPU-accelerated grid search library [12] is created that searches through the user-defined space of candidate trajectory models seeking the trajectory minimizes the performance function of equation (2).

Experimental work has shown that focusing algorithms are highly sensitive to variation in the slope and curvature parameters. As such, these parameters are sampled at a density sufficient to detect coherence. For linear linear trajectories this leads to a solution space consisting of trajectories constrained to lie within a 3D cone. For quadratic trajectories this leads to a solution space having a shape corresponding to a generalized cylinder with quadratic space-curve axis and linearly increasing circular cross section, e.g., a cone with quadratically-bent axis.

In our application we consider a vehicle having unknown velocities and consider using the trajectory estimate as an update to the system state. In such contexts the size of the search space would be proportional to the uncertainty associated with the current state of the vehicle. This uncertainty is typically provided by the guidance, navigation, and control (GNC) filter, which integrates sensor measurements and other data to estimate the vehicle's position, velocity, and orientation. Solutions found via our approach could then be used as feedback to the onboard GNS system as an independent source of velocity and position measurements.

We found that GPU implementation of the search required significant GPU device resources to be dedicated to each trajectory solution. For this reaons we utilized CUDA streams to evaluate the quality of each trajectory. Using CUDA streams, each trajectory evaluation problem will be given the resources needed to focus the SAR image as they become available which maximizes GPU utilization without exceeding the compute resources of the GPU device.

CUDA streams return the value of the column entropy given a guessed trajectory and a final very quick CUDA kernel is required to find the minimum value of the column entropy for all for all trajectory models in the search space which is taken as the final solution. Our results show the focused SAR image using the final solution.

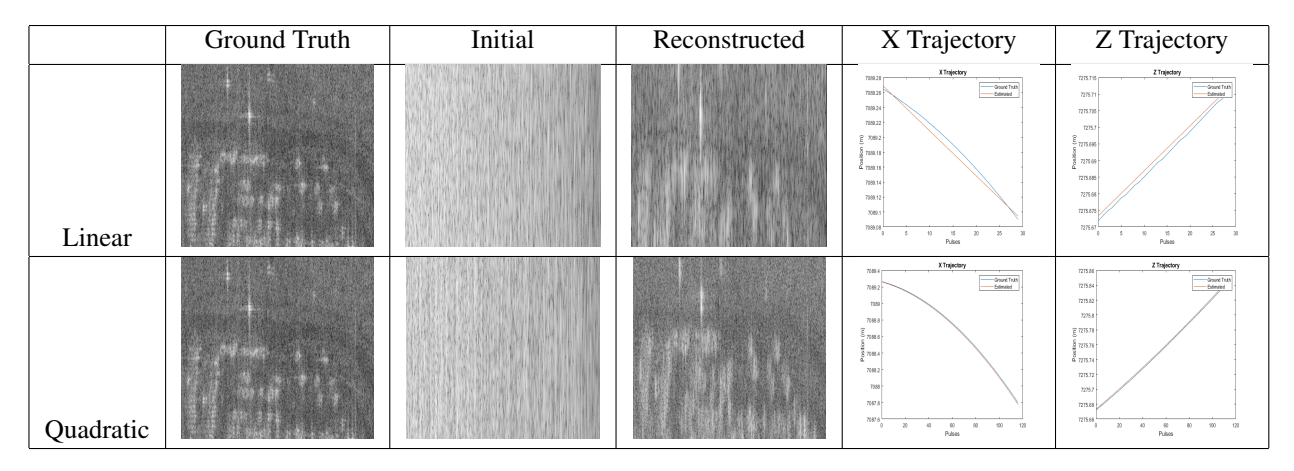


**Table 1**: Linear and quadratic models are shown in rows 1 and 2 of the table. The first three columns from left to right depict the SAR images for: (a) the ground truth trajectory, (b) an incorrect trajectory, (c) reconstructed trajectory. The final two columns plot the estimated X (left) and Z (right) position relative to ground truth for the 30 and 117 pulses considered.

## 4 Results

Linear and quadratic parametric models were considered for estimating the trajectory of the 3D space curve models. For the linear model, the grid search space for the linear coefficients were  $\pm 2.6m$  of the ground truth coefficients with 23 samples each for the X,Y, and Z axis and a velocity search of 90% to 110% with 5 samples (60,835 candidate trajectories total). For the quadratic model, the grid search space modified the linear and quadratic coefficients for  $\pm 1.3m$  with 5 samples each for the X,Y, and Z axis with a velocity search of 90% to 110% with 5 samples each (78,125 candidate trajectories total). The experiments were performed on a system containing an Intel Xeon Silver 4110, NVIDIA RTX A6000 48 GB, and 160 GB RAM which was capable of processing 2671.3 linear candidate trajectories per second and 1827.7 quadratic candidate trajectories per second.

Raw backscatter signals and trajectories from the GOTCHA dataset [13] served as ground truth and phase history data. This dataset contains X-band data spanning 360 degrees of azimuth across 8 elevation angles and 4 polarization states. The experiment operated on 8 azimuth degrees (0° to 315°), 8 elevation angles, and the 4 polarization states. The procedure followed the same steps as above with 60,835 candidate trajectories for the linear model and 78,125 candidate trajectories for the quadratic model.

Table 1 and Table 2 depict trajectory estimation results for linear trajectory and quadratic trajectory models. The linear trajectory considered 30 pulses for estimation and the quadratic trajectory considered 117 pulses for estimation. Representative trajectory X and Z positions are shown in the leftmost columns and the focused SAR images associated with the final trajectory estimates are shown in the column labeled "Reconstructed." Table 2 contains additional examples of the algorithm results for both the linear and quadratic models for other elements of the GOTCHA dataset.

# 5 Conclusion

This article describes a massively parallel approach to solve the NP-hard problem of focusing radar data collected in the presence of excessively large motion errors. Little research has been dedicated to the development of focusing algorithms capable of image formation for large magnitude motion error and advancement mainly because it is a non-deterministic polynomial-time hard problem. We proposed an approach by minimizing the dimension and size of the search space and searching for a candidate solution using a massively parallel GPU search. By parameterizing the trajectory and searching over the coefficients of the parameters and using the total column entropy function, we were able to focus SAR images by finding the satisfactory candidate trajectory from the grid search space.

## 6 References

- [1] Michael Israel Duersch, *Backprojection for Synthetic Aperture Radar*, Ph.D. thesis, Brigham Young University, 2013.
- [2] Aaron Evers and Julie Ann Jackson, "A comparison of autofocus algorithms for backprojection synthetic aperture radar," in 2020 IEEE International Radar Conference (RADAR). apr 2020, IEEE.
- [3] Orhan Arikan and David C. Munson, "A tomographic formulation of bistatic synthetic aperture radar," in *Advances in Communications and Signal Processing*, pp. 289–302. Springer Berlin Heidelberg, 1989.
- [4] C. Wu, "A digital system to produce imagery from SAR data," in *System Design Driven by Sensors*. aug 1976, American Institute of Aeronautics and Astronautics.
- [5] B.D. Rigling and R.L. Moses, "Polar format algorithm

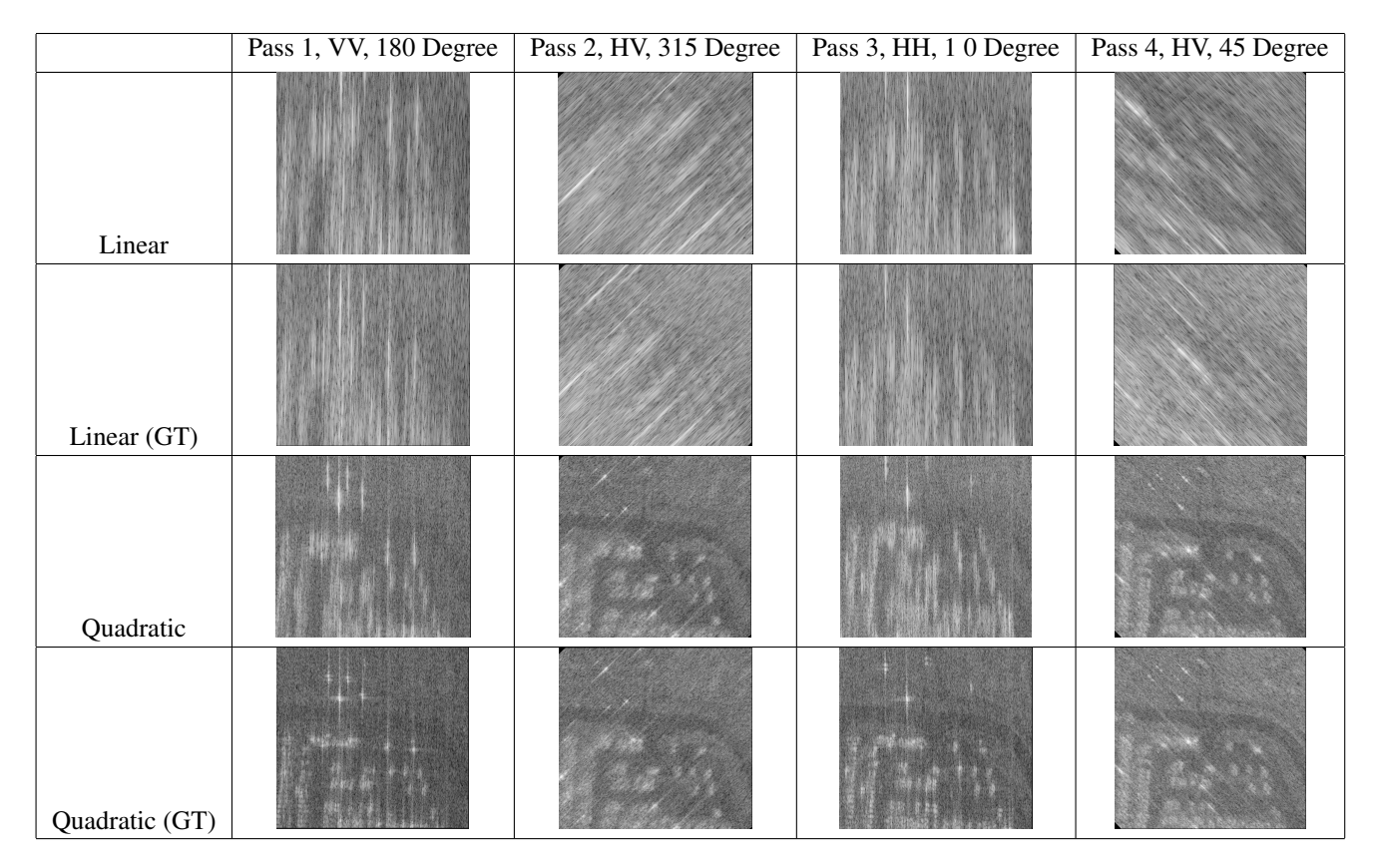


Table 2: Examples of the linear and quadratic models focused SAR images from the GOTCHA dataset and their respective ground truth coefficient images.

- for bistatic SAR," *IEEE Transactions on Aerospace and Electronic Systems*, vol. 40, no. 4, pp. 1147–1159, oct 2004.
- [6] R.K. Raney, H. Runge, R. Bamler, I.G. Cumming, and F.H. Wong, "Precision SAR processing using chirp scaling," *IEEE Transactions on Geoscience and Remote Sensing*, vol. 32, no. 4, pp. 786–799, jul 1994.
- [7] G. Fornado, "Trajectory deviations in airborne SAR: analysis and compensation," *IEEE Transactions on Aerospace and Electronic Systems*, vol. 35, no. 3, pp. 997–1009, jul 1999.
- [8] G. Fornaro, E. Sansosti, R. Lanari, and M. Tesauro, "Role of processing geometry in SAR raw data focusing," *IEEE Transactions on Aerospace and Electronic* Systems, vol. 38, no. 2, pp. 441–454, apr 2002.
- [9] Michael I Duersch and David G Long, "Analysis of time-domain back-projection for stripmap SAR," *International Journal of Remote Sensing*, vol. 36, no. 8, pp. 2010–2036, apr 2015.
- [10] Aaron Evers and Julie Ann Jackson, "A generalized phase gradient autofocus algorithm," *IEEE Transactions on Computational Imaging*, vol. 5, no. 4, pp. 606–619, dec 2019.

- [11] D.C. Munson, J.D. O'Brien, and W.K. Jenkins, "A tomographic formulation of spotlight-mode synthetic aperture radar," *Proceedings of the IEEE*, vol. 71, no. 8, pp. 917–925, 1983.
- [12] Chris Beam and Andrew Willis, "cugrid-search," https://https://github.com/uncc-visionlab/cuGridSearch, 2022.
- [13] "Gotcha volumetric sar data set, version 1.0," Jan. 2021, [Online; Accessed 6-November-2021].